American Control Conference
June 1987, Minneapolis, Minnesota, USA

Acc 87

Design and Control of the Active Compliant End-Effector

H. Kazerooni
J. Guo
Mechanical Engineering Department
University of Minnesota
Minneapolis, MN 55455

Abstract

The design, construction and control of a wide bandwidth, active end-effector which can be attached to the end-point of a commercial robot manipulator is presented here. Electronic compliancy (Impedance Control) [11] has been developed on this device. The end-effector behaves dynamically as a two-dimensional, Remote Center Compliance (RCC). The compliancy in this active end-effector is developed electronically and can therefore be modulated by an on-line computer. The device is a planar, five-bar linkage which is driven by two direct drive, brush-less DC motors. A two-dimensional, piezoelectric force cell on the end-point of the device, two 12-bit encoders, and two tachometers on the motors form the measurement system for this device. The high structural stiffness and light weight of the material used in the system allows for a wide bandwidth Impedance Control.

Nomenclature

E	environment dynamics
e	input trajectory
f	contact force
G	closed-loop transfer function matrix
H	the compensator
j	complex number notation $\sqrt{-1}$
J_c	Jacobian
J_i	moment of inertia of each link relative to the end-point of the link
K	stiffness matrix
l_i, m_i	length and mass of each link
M_o	inertia matrix
S	sensitivity transfer function matrix
r	input command vector
$T=[T_1\ T_2]^T$	torque vector
$X=[X_t\ X_n]^T$	vector of the tool position in the cartesian coordinate frame
X_o	environment position before contact
x_i, θ_i	location of the center of mass and orientation of each link
α	small perturbation of θ_1 in the neighborhood of $\theta_1 = 90^o$
δe	end-point deflection in X_n-direction
ω_d	dynamic manipulability
ω_o	frequency range of the operation (bandwidth)

1. Introduction

Manufacturing manipulations require mechanical interaction with the environment or with the object being manipulated. Robot manipulators are subject to interaction forces when they maneuver in a constrained work-space. Inserting a computer board in a slot or deburring an edge are examples of constrained maneuvers. In constrained maneuvers, one is concerned with not only the position of the robot end-point, but also the contact forces. In constrained maneuvering, the interaction forces must be accommodated rather than resisted. If we define compliancy as a measure of the ability of the manipulators to react to interaction forces and torques, the objective is to assure compliant motion (passively or actively) for the robot end-point in the cartesian coordinate frame for manipulators that must maneuver in the constrained environments.

An example of the manufacturing manipulation that requires compliancy is robotic assembly. To perform the assembly of parts that are not perfectly aligned, one must use a compliant element between the part and the robot to ease the insertion process. The RCC is a device that can be attached to the end-point of the robot manipulators [3,20]. This device develops a passive compliant interface between the robot and the part. The primary function of the RCC is to act as a filter that decreases the contact force between the part and the robot due to the robot oscillations, robot programming error, and part fixturing errors. These end-effectors are called passive because the elements that generate compliancy are passive and no external energy is flowing into the system. The need for variable compliant end-effectors is a motivation for development of the active compliant end-effector. Robotic deburring [8,9,10] is an example of a manufacturing task that requires the modulation of the end-point compliancy with an on-line computer. The modulation of the end-point compliancy (impedance in our case) depends on the geometry of the edge of the part to be deburred. The impedance of the end-point must be modulated continuously when the robot travels around the edge of the part. The details of this problem is given in references 8,10,12.

Active end-effectors are devices that can be mounted at the end-point of the robot manipulators to develop more degrees of freedom [5]. The active end-effector can be used as a compliant tool holder. There is no passive compliant element in the system, because the compliancy in

the system is generated electronically [6,7,11]. The advantage of this system over other passive systems is that one can modulate the compliancy in the system arbitrarily by an on-line computer, depending on the requirements of the tasks. Two DC actuators power the two degrees of freedom of the system.

2. Architecture

Figure 1 and 2 show the schematic diagram of the active end-effector.

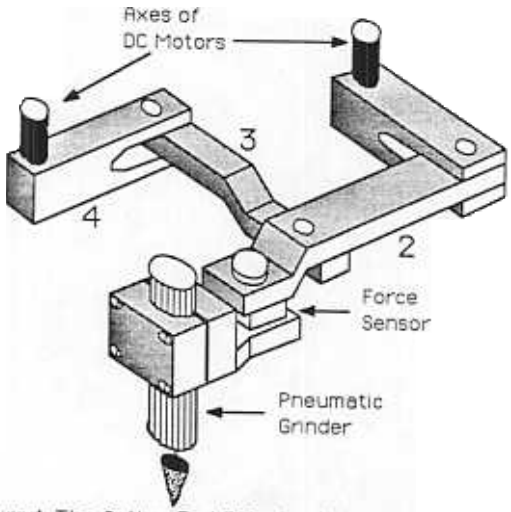

Figure 1: The Active End-Effector Holding a Pneumatic Grinder

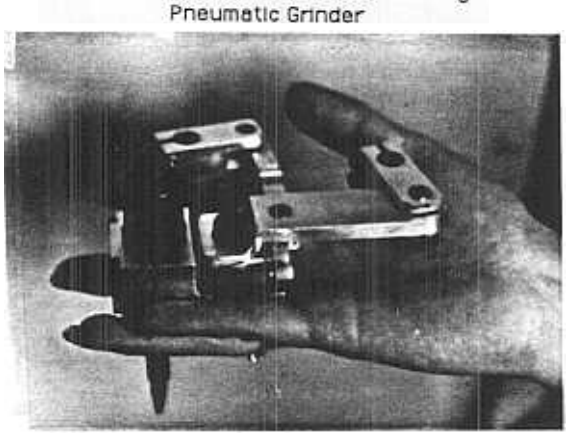

Figure 2: The Active End-Effector

The end-effector is a 5-bar linkage with two degrees of freedom. All are articulated drive joints. The links are made of Aluminium 6061. The actuators are DC brush-less direct drive motors equipped with 12 bit encoders and tachometers. The choice of the direct drive system eliminates backlash and develops more structural rigidity in the system. This structural rigidity allows for a wide control bandwidth and higher precision. The stall torque and the peak torque for each motor is 5 lb-in and 20 lb-in, respectively. Each motors weighs 2.4 lbs. A wide-bandwidth piezoelectric-based force sensor is located between the end-point of the mechanism and the end-effector gripper to measure the force on the tool. The force sensor is pre-loaded by a clamping bolt, and measures the force in two dimensions in the plane of the mechanism. The entire weight of the links with bearings and force sensor is 111.4 grams. The end-effector can be attached to the robot manipulator by a simple fixture between the housing of the motors and the robot end-point. Figure 3 shows the side view of the end-effector.

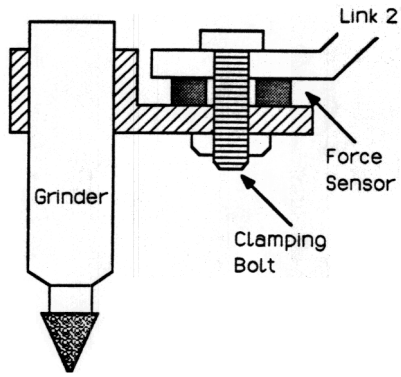

Figure 3: The Side View of the Force Sensor Assembly

The characteristics of this end-effector are as follows:
Size of the 5-bar linkage at nominal position 2.167"×4.160"
The height of the end-effector with motors (excluding the grinder tool).....3.760"
Linear work-space of the end-point.....0.3" ×0.3"
Resolution of the end-point motion.....2.6×10^{-3} "
Bandwidth of the control system.....25 hertz
Total mass of the mechanism (without the tool)....0.25 lb.
Weight of two motors.....4.8 lb.
Weight of the tool.....0.3 lb.
Total mass (mass of the mechanism and the motors, excluding the grinding tool).....5.05 lb.

3. Design

In this section two significant properties of this end-effector are explained. Although the active end-effector can be used as a micro-positioning system for small and fast maneuvering of the tool, it is designed to act as an RCC. The end-point of the end-effector behaves as if there are two orthogonal springs holding the tool.

In this behavior, the end-point motion is very small. Equation 1 describes the dynamic behavior of the mechanism, for small perturbation of the mechanism around its nominal point in absence of the centrifugal and coriolis forces. We will justify the absence of centrifugal and coriolis forces in the dynamic equation of the system in our analysis.

$$\ddot{X} = J_c M_o^{-1} T \qquad (1)$$

Where:

$X = [X_t \;\; X_n]^T$.....2×1 vector of the tool position in the cartesian coordinate frame
J_c..... 2×2 Jacobian matrix
M_o..... 2×2 mass matrix
$T = [T_1 \;\; T_2]^T$..... 2×1 vector of the motor torque

$J_o M_o^{-1}$ is a transmission ratio between the actuator torque and the end-point acceleration. This matrix is function of joint angles. It is desirable to operate the

end-effector in an orientation such that $J_c M_o^{-1}$ is almost constant or has minimum rate of change. The general form M_o and J_c are given in Appendix A by equations A1 and A2. Figure A1 in Appendix A shows a five-bar linkage in the general form. The device is designed to operate around the neighborhood of the nominal orientation of $\theta_1 = 90°$, $\theta_2 = 0°$, $\theta_3 = 90°$ and $\theta_4 = 180°$ as shown in Figure 4. θ_1 and θ_4 are the driving angles, and we intend to drive the system such that $85° < \theta_1 < 95°$ and $175° < \theta_4 < 185°$, (Total of ±5° deviation from their nominal values). It can be shown that the rate of change of $J_c M_o^{-1}$ at this nominal orientation is minimum. The dynamic manipulability, ω_d is defined as the square root of the multiplication of the maximum and minimum singular values of $J_c M_o^{-1}$ [19]. ω_d measures the rate of change of $J_c M^{-1}$.

$$\omega_d = \sqrt{\sigma_{max}(J_c M_o^{-1})\ \sigma_{min}(J_c M_o^{-1})} \qquad [2]$$

or equivalently:

$$\omega_d = \sqrt{\det(J_c M_o^{-1} M_o^{-T} J_c^T)}$$

ω_d is plotted in Figure 5 as a function of perturbations on θ_1 and θ_4. The perturbation around the nominal values of θ_1 and θ_4 are called $\delta\theta_1$ and $\delta\theta_4$.

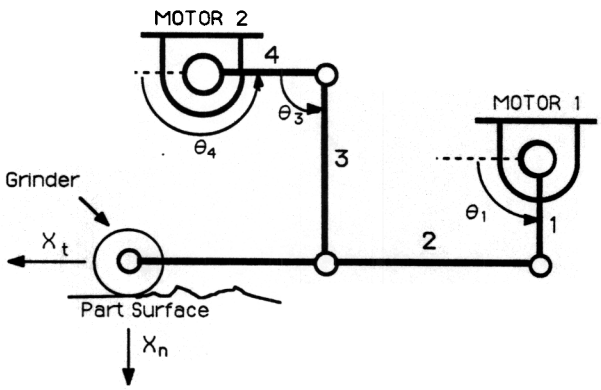

Figure 4: The End-Effector at its Nominal Position $\theta_1 = 90°$ and $\theta_4 = 180°$

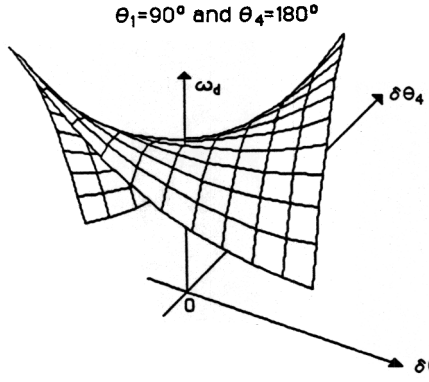

Figure 5: Dynamic Manipulability as a Function of $\delta\theta_1$ and $\delta\theta_4$

According to Figure 5, ω_d is "smooth" for all small perturbations around nominal values of θ_1 and θ_4. Inserting $\theta_1 = 90°$, $\theta_2 = 0°$, $\theta_3 = 90°$ and $\theta_4 = 180°$ into equations A1 and A2 (from Appendix A) results in diagonal matrices for J_c and M_o such that $J_c M_o^{-1}$ is diagonal and also has the minimum rate of change when θ_1 and θ_4 vary slightly from their nominal values. Note that the plot in Figure 5 shows only that at the shown configuration, $J_c M_o^{-1}$ has the minimum rate of change and this allows us to use equation 1 as our dynamic model for the active end-effector. Since the rate of change of $J_c M_o^{-1}$ is minimum at the nominal configuration, centrifugal and coriolis forces can be neglected from the dynamic equations of the end-effector. (These terms are functions of the rate of change of the inertia matrix). If the end-effector is considered in another configuration, then any slight perturbation of the driving joints will develop significant change in $J_c M_o^{-1}$ and consequently, non-linearity will be developed in the dynamic behavior of the system. Since $J_c M_o^{-1}$ is a diagonal matrix, then the dynamic equation of the end-effector is uncoupled. Based on this uncoupling, for a limited range, motor 1 maneuvers the end-point in X_t-direction, while motor 2 moves the end-point independently in the X_n-direction.

We use the end-effector in the configuration shown in Figure 4. All the links are orthogonal to one another. If θ_1 is perturbed from its nominal value as much as α, then the value of the end-point perturbation in the X_n direction, δe, can be calculated form equation 3. Figure 6 shows the configuration of the perturbed system.

$$\delta e = \frac{l_1}{2 l_2}\,\alpha^2 \left(l_5 - l_2 - \frac{l_1 l_5}{l_3} \right) \qquad [3]$$

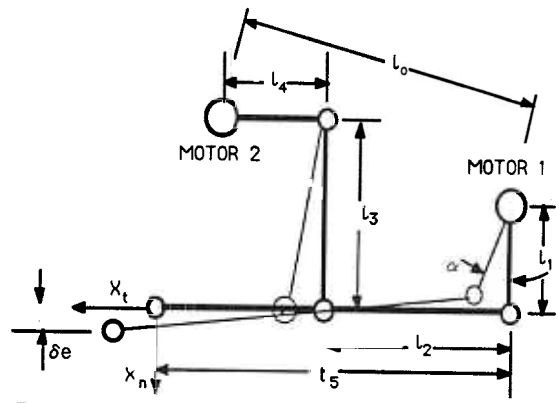

Figure 6 : The 5-bar Mechanism with Small Deflection of α

For $\delta e = 0$, the following equality must be satisfied.

$$l_5 - l_2 = \frac{l_1 l_5}{l_3} \qquad [4]$$

By satisfying equation 4, we choose the lengths of the mechanism such that the end-point of the end-effector always moves along the X_t axis for small value of α. ($\alpha < \pm 5°$) This configuration is an application of the well-known Watt's [22] straight-line mechanism. This property is attractive for deburring purposes. According to the references [8,10], the end-effector must be very stiff in the direction normal to the part and compliant in the direction tangential to the part. Once the grinder encounters a burr, motor 1, which is responsible for motion

in the X_t-direction, moves the tool backward to decrease the amount of the force. In the deburring process, motor 1 constantly moves the end-point back and forth in the X_t-direction. If equation 4 is guaranteed, then the motion of the end-point in the X_t-direction does not affect the motion of the tool in the X_n-direction. The kinematic independence of the end-point motion in X_n-direction from the motion of the end-point in X_t-direction allows for a very smooth surface finish for deburring purposes. The following constraints are sufficient to result in the exact lengths of the mechanism:

- Equation 4 must be satisfied.
- For simplicity in design and construction, $l_1=l_4$ and $l_3=l_2$
- l_o=3" (Each actuator has 1.375" radius)
- l_4 must be such that if $\delta\theta_4=5^o$, the amount of motion in X_n-direction is 0.15".

The above five constraints are sufficient conditions to result the lengths of the five links. Using the triangle equality and some algebra, the following lengths are calculated:

l_o=3", l_1 = 0.906", l_2= 1.917", l_3=1.917" and l_4=0.906"

4. Electronic Compliancy

First we frame the controller design objectives by a set of meaningful mathematical terms; then we give a summary of the controller design method to develop compliancy for linear systems. The complete description of the control method to develop electronic compliancy (impedance control) for an n degree of freedom non-linear manipulative system is given in reference 11.

The controller design objective is to provide a stabilizing dynamic compensator for the system such that the ratio of the position of end-point of the end-effector to an interaction force is constant within a given operating frequency range. (The very general definition is given in references 6 and 7). The above statement can be mathematically expressed by equation 5.

$$\delta F(j\omega) = K\,\delta X(j\omega) \qquad \text{for all } 0<\omega<\omega_o \qquad (5)$$

where:

$\delta F(j\omega)$ = 2×1 vector of the deviation of the interaction forces from their equilibrium value in the global cartesian coordinate frame.

$\delta X(j\omega)$ = 2×1 vector of the deviation of the end-point position from the nominal point in the global cartesian coordinate frame.

K = 2×2 real-valued, non-singular diagonal stiffness matrix with constant members.

ω_o = bandwidth (frequency range of operation)

j = complex number notation, $\sqrt{-1}$

The stiffness matrix is the designer's choice which, depending on the application, contains different values for each direction. By specifying K, the designer governs the behavior of the end-effector in constrained maneuvers. Large elements of the K-matrix imply large interaction forces and torques. Small members of the K-matrix allow for a considerable amount of motion in the end-effector in response to interaction forces. Even though a diagonal stiffness matrix is appealing for the purpose of static uncoupling, the K-matrix in general is not restricted to any structure.

Mechanical systems are not generally responsive to external forces at high frequencies. As the frequency increases, the effect of the feedback disappears gradually, (depending on the type of controller used), until the inertia of the system dominates its overall motion. Therefore, depending on the dynamics of the system, equation 5 may not hold for a wide frequency range. It is necessary to consider the specification of ω_o as the second item of interest. In other words, two independent issues are addressed by equation 5: first, a simple relationship between $\delta F(j\omega)$ and $\delta X(j\omega)$; second, the frequency range of operation, ω_o, such that equation 5 holds true. Besides choosing an appropriate stiffness matrix, K, and a viable ω_o, a designer must also guarantee the stability of the closed-loop system.

We consider the architecture of Figure 7 as the closed-loop control system for the end-effector. The detailed description of each operator in Figure 7 is given in reference 11. Since the dynamic behavior of the end-effector in the neighborhood of its operating point is linear, all the operators in Figure 7 are considered transfer function matrices. In the general approach for development of compliancy in reference 11, E, G, H and S are non-linear operators.

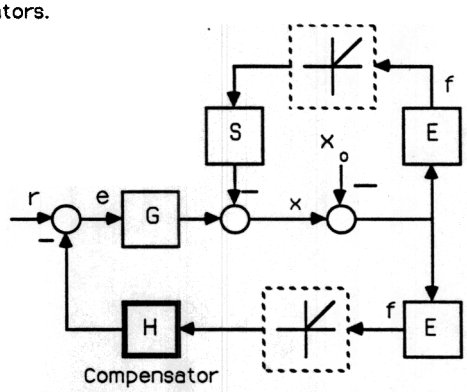

Figure 7: The Closed-Loop Control for the End-Effector

G is the transfer function matrix that represents the dynamic behavior of the manipulative system (end-effector in our case) with a positioning controller. The input to G is a n×1 vector of input trajectory, e. The fact that most manipulative systems have some kind of positioning controllers is the motivation behind our approach. One can use great number of methodologies for the development of the robust positioning controllers [14,15,18] G can be calculated experimentally or analytically. Note that G is approximately equal to the unity matrix for the frequencies within its bandwidth. S is the sensitivity transfer function matrix. S represents the relationship between the external force on the end point of the end-effector and the end-point motion. This motion is due to either structural compliance in the end-effector mechanism or the positioning controller compliance. For good positioning system S is quite "small". (The notion of "small" can be regarded in the singular value sense when S is a transfer function matrix. L_p-norm **[18,19]** can be considered to show the size of S in the non-linear case.) E represents the dynamic behavior of the environment. Readers can be convinced of role of E by analyzing the relationship of the force and displacement of a spring as a simple model of the environment. H is the compensator to

be designed. The input to this compensator is the contact force. The compensator output signal is being subtracted from the vector of input command, r, resulting in the error signal, e, as the input trajectory for the robot manipulator. r is the input command vector which is used differently for the two categories of maneuverings; as a trajectory command to move the end-point in unconstrained space and as a command to shape the contact force in the constrained space. When the manipulative system and environment are in contact, then the value of the contact force and the end-point position of the robot are given by equations 6 and 7.

$$f=E[I+SE+GHE]^{-1}Gr \qquad (6)$$

$$y=(I+SE+GHE)^{-1}Gr \qquad (7)$$

The general goal is to choose a class of compensator, H, to shape the impedance of the system, $E[I+SE+GHE]^{-1}G$, in equation 6. When the system is not in contact with the environment, the actual position of the end-point is equal to the input trajectory command within the bandwidth of G. (Note that G is approximately equal to unity matrix within its bandwidth.) When the system is in contact with the environment, then the contact force follows r according to equation 6. We do not command any set-point for force as we do in admittance control [13,21]. This method is called Impedance Control [4,6,7] because it accepts a position vector as input and it reflects a force vector as output. There is no hardware or software switch in the control system when the robot travels from unconstrained space to constrained space. The feedback loop on the contact force closes naturally when the robot encounters the environment. When the system is contact with the environment, then the contact force is a function of r according to equation 6. This compensator must also guarantee the stability of the system.

We are interested in a particular case when r=0. Suppose the environment is being moved into the end-effector or the end-effector is being moved into the environment. This is the case that occurs in robotic deburring. The relation between the contact force and the end-point deflection is given by equation 8 if E approaches ∞ in the singular value sense. (This is shown in reference 11)

$$f=(S+H)^{-1}x \qquad (8)$$

Equality 8 is derived by inspection of the block diagram in Figure 7. The fact that in most manufacturing tasks such as robotic deburring, the end point of the system is in contact with a very stiff environment, is the motivation behind our consideration in development of equation 8. $(S+H)^{-1}$ is similar to the stiffness matrix, K which is defined by equation 5. By selecting the value of H and knowledge of S one can select the members of H such that $(S+H)^{-1}$ of equation 8 meets the deburring requirements as given by equation 5. A set of experiments is given in reference 12 to clarify the control method.

7. Summary and Conclusion

An active end-effector with controllable, compliant motion (Electronic Compliancy) has been designed, built, and tested for robotic operations. The active end-effector (unlike the passive system) does not contain any spring or dampers. The compliancy in the active end-effector is developed electronically and therefore can be modulated by an on-line computer. The active end-effector allows for compensation of the robot's position uncertainties from fixturing errors, robot programing resolution, and robot oscillations. This fully instrumented end-effector weighs only 5.05 lbs. and can be mounted at the end-point of the commercial robot manipulator. Two state-of-the-art miniature actuators power the end-effector directly. The high stiffness and light weight of the material used in the system allows for a wide bandwidth Impedance Control. A miniature force cell measures the forces in two dimensions. The tool holder can maneuver a very light pneumatic grinder in a linear work-space of about 0.3"x0.3". The measurements taken on the mechanism are contact forces, angular velocities, and the orientation of the mechanism. Satisfying a kinematic constraint for this end-effector allows for uncoupled dynamic behavior for a bounded range.

Appendix A

This appendix is dedicated to deriving the Jacobian and the inertia matrix of a general five-bar linkage. In Figure A1, J_i, l_i, x_i, m_i and θ_i represent the moment of inertia relative to the end-point, length, location of the center of mass, mass and the orientation of each link for i= 1,2,3 and 4.

Using the standard method in [1], the Jacobian of the linkage can be represented by equation A1.

$$J_o = \begin{bmatrix} J_{11} & J_{12} \\ J_{21} & J_{22} \end{bmatrix} \qquad (A1)$$

where:

$J_{11} = -l_1 \sin(\theta_1) + a\, l_5 \sin(\theta_2)$
$J_{21} = l_1 \cos(\theta_1) - a\, l_5 \cos(\theta_2)$
$J_{12} = -b\, l_5 \sin(\theta_2)$
$J_{22} = b\, l_5 \cos(\theta_2)$

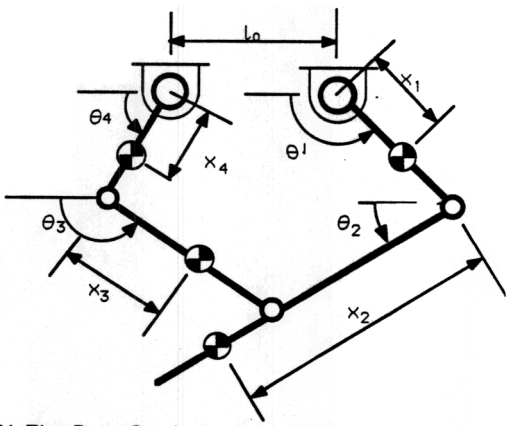

Figure A1: The Five Bar Linkage in the General Form

The mass matrix is given by equation A2.

$$M = \begin{bmatrix} M_{11} & M_{12} \\ M_{21} & M_{22} \end{bmatrix} \qquad (A2)$$

Where:

$M_{11} = J_1 + m_2 l_1^2 + J_2 a^2 + J_3 c^2 + 2 x_2 l_1 \cos(\theta_1 - \theta_2) a m_2$

$M_{12} = J_2 a b + b \cos(\theta_1 - \theta_2) x_2 l_1 m_2 + J_3 c d + c \cos(\theta_4 - \theta_3) x_3 l_4 m_3$

$M_{21} = M_{12}$

$M_{22} = 2 m_3 l_4 x_3 d \cos(\theta_4 - \theta_3) + J_3 d^2 + J_4 + m_3 l_4^2 + J_2 b^2$

a, b, c, d are given below.

$a = l_1 \sin(\theta_1 - \theta_3) / \{ l_2 \sin(\theta_2 - \theta_3) \}$

$b = l_4 \sin(\theta_4 - \theta_3) / \{ l2 \sin(\theta_2 - \theta_3) \}$

$c = l_1 \sin(\theta_1 - \theta_2) / \{ l_3 \sin(\theta_2 - \theta_3) \}$

$d = l_4 \sin(\theta_4 - \theta_2) / \{ l_3 \sin(\theta_2 - \theta_3) \}$

References

1) Asada, H., Slotine, J. J. E., "Robot Analysis and Control", John Wiley and Sons.

2) Bausch, J., Kramer, B., Kazerooni, H., "The Development of the Compliant Tool Holders for Robotic Deburring", ASME Winter Annual Meeting, December 1986, Anaheim, California.

3) Drake, S. H., "Using Compliance in Lieu of Sensory Feedback for Automatic Assembly", IFAC Symposium of Information and Control Problems in Manufacturing Technology, Tokyo, 1977.

4) Hogan, N., "Impedance Control: An Approach to Manipulation, Part 1: Theory, Part 2: Implementation, Part 3: Applications", ASME Journal of Dynamic Systems, Measurement, and Control, 1985.

5) Hollis, R. L., "A Planar XY Robotic Fine Positioning Device", In proceedings of the IEEE International Conference on Robotics and Automation, St. Louis, Missouri, March 1985.

6) Kazerooni, H., Houpt, P. K., Sheridan, T. B., "Fundamentals of Robust Compliant Motion for Manipulators" ,IEEE Journal of Robotics and Automation , N2, V2, June 1986.

7) Kazerooni, H., Houpt, P. K., Sheridan, T. B., "A Design Method for Robust Compliant Motion of Manipulators", IEEE Journal of Robotics and Automation .N2, V2, June 1986.

8) Kazerooni, H., Bausch, J. J., Kramer, B., "An Approach to Automated Deburring by Robot Manipulators", ASME Journal of Dynamic Systems, Measurements and Control, December 1986.

9) Kazerooni, H., Bausch, J. J., Kramer, B., "An approach to Robotic Deburring" , In proceedings of American Control Conference , Seattle, June 1986.

10) Kazerooni, H., "Automated Robotic Deburring Using Electronic Compliancy; Impedance Control", In Proceedings of the IEEE International Conference on Robotics and Automation, Raleigh, North Carolina, March 1987.

11) Kazerooni, H., Baikovicius, J., Guo, J.,"Compliant Motion Control for Robot Manipulators", In proceedings of the American Control Conference, Minneapolis, June 1987.

12) Kazerooni, H., Guo, J.,"Direct-Drive Active Compliant End-Effector (Active RCC)", In Proceedings of the IEEE International Conference on Robotics and Automation, Raleigh, North Carolina, March 1987.

13) Raibert, M. H., Craig, J. J., "Hybrid Position/Force Control of Manipulators", ASME Journal of Dynamic Systems, Measurement, and Control. June 1981.

14) Slotine, J. J. , "Sliding Controller Design for Non-Linear Systems", International Journal of Control, V40, N2, 1984.

15) Slotine, J. J., "The Robust Control of Robot Manipulators", The International Journal of Robotics Research, V4, N2, 1985.

16) Vidyasagar, M., "Non-Linear Systems Analysis", Prentice-Hall.

17) Vidyasagar, M., Desoer, C. A., "Feedback Systems: Input-Output Properties", Academic Press.

18) Vidyasagar, M., Spong, M. W., "Robust Non-Linear Control of Robot Manipulators", IEEE Conference on Decision and Control", December 1985.

19) Yoshikawa, T., "Dynamic Manipulability of Robot Manipulators", Journal of Robotic Systems, Volume 2, Number 1, 1985.

20) Watson, P. C.,"A Multidimensional System Analysis of the Assembly Process as Performed by a Manipulator", in Proceedings of the First American Robot Conference, Chicago, 1976.

21) Whitney, D. E., "Force-Feedback Control of Manipulator Fine Motions", ASME Journal of Dynamic Systems, Measurement, and Control, June, 1977.

22) Rappaport, S., "Five-bar Linkage for Straight Line Motion", Product Engineering, October 1959.